Arabian Journal of Chemistry (2023) **16**, 104720

King Saud University

Arabian Journal of Chemistry

www.ksu.edu.sa
www.sciencedirect.com

ORIGINAL ARTICLE

Establishing TA-Pb/Cu and SA-Pb/Cu interface catalyst shells on HMX surfaces via *in situ* coprecipitation to ameliorate the performances of HMX

Guanchao Lan [a,b], Guoliang Jin [b], Jian Ruan [b], Xinping Zhao [b], Jianlong Wang [a], Jing Li [c,*]

[a] *School of Chemistry and Chemical Engineering, North University of China, Taiyuan 030051, China*
[b] *Gansu Yin Guang Chemical Industry Group Co. Ltd., Baiyin 730900, China*
[c] *School of Materials Science and Engineering, North University of China, Taiyuan 030051, China*

Received 2 October 2022; accepted 21 February 2023
Available online 27 February 2023

KEYWORDS

HMX;
Composites;
In situ coprecipitation;
Surface catalysis

Abstract Lead/copper tannate (TA-Pb/Cu) and lead/copper salicylate (SA-Pb/Cu) interface catalyst shells are established on the surface of 1,3,5,7-tetranitro-1,3,5,7-tetrazacyclooctane (HMX) via *in situ* coprecipitation to prepare HMX@TA-Pb/Cu and HMX@SA-Pb/Cu composites. The structures and properties of the obtained HMX@TA-Pb/Cu and HMX@SA-Pb/Cu composites are characterized in detail. Molecular dynamics simulations are performed to study the adsorption mechanism of TA-Pb/Cu and SA-Pb/Cu on HMX surface. The residues after HMX@TA-Pb/Cu and HMX@SA-Pb/Cu combusted in air are collected and characterized to study the catalytic effect of TA-Pb/Cu and SA-Pb/Cu on combustion. The study results show that TA-Pb/Cu shells are coated on HMX surface due to the excellent membrane-forming properties of TA, while SA-Pb/Cu shells are embedded in the gullies and holes of HMX surface. TA-Pb/Cu and SA-Pb/Cu shells can decrease the mechanical sensitivities and catalyze the decomposition and combustion of HMX, and the catalytic effects of *in situ* coprecipitation are better than that of physical mixing. In addition, the phase transition temperature of HMX in HMX@TA-Pb/Cu is increased while that of

* Corresponding author.
E-mail address: 20210064@nuc.edu.cn (J. Li).
Peer review under responsibility of King Saud University.

Production and hosting by Elsevier

https://doi.org/10.1016/j.arabjc.2023.104720

HMX@SA-Pb/Cu is decreased, illustrating that TA-Pb/Cu can enhance the thermal stability of HMX while SA-Pb/Cu can catalyze the phase transition of HMX.

1. Introduction

Over the past few decades, 1,3,5,7-tetranitro-1,3,5,7-tetrazacyclooctane (HMX, Fig. 1a) is one of the most widely used energetic materials in high energy weapon warhead and composite modified double base (CMDB) propellants, because it successfully combines a relatively low cost with excellent energetic characteristics such as high enthalpy of formation, high density, high detonation velocity and high thermal stability (Kosareva et al., 2022; Klapötke, 2018). Accompany with excellent energy properties, HMX exhibits a considerably higher mechanical sensitivity that restricts its handling, transportation, and processing (Kosareva et al., 2022). Therefore, many researchers focus on decreasing the sensitivity of HMX through recrystallization, exploring HMX cocrystals, preparing microcapsules via *in situ* coating, *etc* (An et al., 2014; Hou et al., 2018; Elbasuney et al.; Bolton and Matzger, 2011; Lin et al., 2019; Yang et al., 2015; Li et al., 2020; Gong et al., 2017). Among these techniques, *in situ* coating is an efficient method because *in situ* chemical reaction can facilitate extraordinarily high coverage on HMX surfaces (Yang et al., 2015; Lan et al., 2022). In addition, the thermal and combustion performances of HMX can be ameliorated by introducing catalytic components to coating materials via *in situ* reaction, which can sufficiently utilize the catalytic effect of catalytic components compared with physical mixing.

Former studies show that lead/copper composites salt can effectively catalyze the combustion property of CMDB propellants (Liu et al., 2001; Jiang et al., 2020). Therefore, both Pb^{2+} and Cu^{2+} are expected to introduce to the surface of HMX via *in situ* reaction. The coating material are expected to decrease the sensitivity and catalyze the combution of HMX. Tannic acid (TA, Fig. 1b), a plant-derived polyphenol bearing multiple pyrogallol groups, can provide noncovalent, reversible, and specific interactions with metal ions (Pb^{2+}, Fe^{3+}, Cu^{2+}, etc.) to form robust metal-phenolic networks film (Li et al., 2020; Xiao et al., 2021; Xiao and Liang, 2021). Under alkaline conditions, TA can react with $Pb(NO_3)_2$ and $Cu(NO_3)_2$ to form TA-Pb/Cu composites catalysts film. For TA-Pb/Cu, there are many unreacted phenolic hydroxyl groups that can form strong hydrogen bond with nitro group of HMX, resulting TA based metal-phenolic networks film can compactly coat on the surface of HMX (Lan et al., 2022). Salicylic acid (SA, Fig. 1c) can react with $Pb(NO_3)_2$ and $Cu(NO_3)_2$ to form SA-Pb/Cu composites salts, which is a common used combustion catalyst of HMX based CMDB propellants (Niu et al., 2022). However, SA-Pb/Cu composites catalysts have few functional groups that can form strong non-bonding interaction with HMX after reaction, resulting in SA-Pb/Cu composites salts are difficult to adsorb on smoothing HMX surface directly. In order to introduce SA-Pb/Cu to HMX surface, it is initial to product roughening treatment of HMX surface to provide more adsorption sites for SA-Pb/Cu.

HMX particles with many gullies are benefit for the adsorption of small molecular material during *in situ* coprecipitation. HMX-DMF complex can be obtained by allowing a warm saturated solution of HMX in DMF to cool to room temperature (Cobbledick and Small, 1975), and the DMF of HMX-DMF complex can be easily removed through stirring in water (Ren, 1994). HMX particles with many holes and gullies can be obtained by removing DMF in HMX-DMF complex. The gullies and holes are ideal adsorption sites for *in situ* deposition coating. In this study, spherical HMX particles with many holes and gullies are first obtained through removing DMF in HMX-DMF complex. Then TA and SA are used to react with lead and copper via *in situ* coprecipitation to prepare HMX@TA-Pb/Cu and HMX@SA-Pb/Cu composites. The performance of HMX@TA-Pb/Cu and HMX@SA-Pb/Cu composites are compared with physical mixtures of HMX/TA-Pb/Cu and HMX/SA-Pb/Cu to study the catalytic effects of *in situ* coprecipitation process.

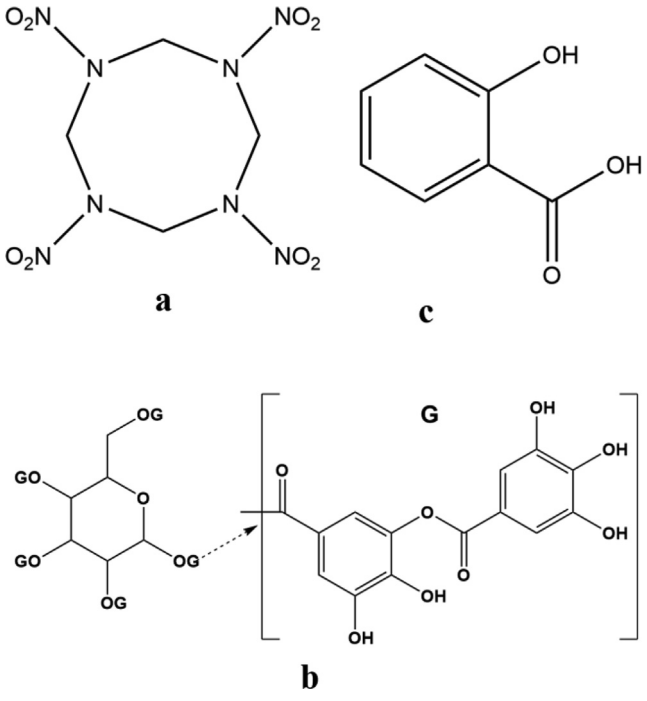

Fig. 1 Molecular structure of HMX (a), TA (b) and SA (c).

2. Experimental details

2.1. Materials

HMX, provided by Gansu Yin Guang Chemical Industry Group Co. Ltd, were purified by recrystallization, and their mass fraction purity was greater than 0.99. TA, SA, *N,N*-dimethylformamide (DMF), acetic acid, sodium laurylsulfonate, lead nitrate, copper nitrate and Tris-Bis were analytical grade and purchased from a local reagent factory without further purification.

2.2. Preparation of HMX particles with high specific surface area

In ambient temperature, 100 g HMX samples was added to 1000 mL DMF, and then heated to 85 °C to dissolve. When HMX particles are completely dissolved, 3.0 g sodium laurylsulfonate was added to the above solution and stirring at 85 °C until the suspension became clearly transparent. Subsequently, 5 g HMX seed crystal was added when the solution was cooled to 80 °C, and stirring 2 h at 80 °C. Then, cool

the suspension to 20 °C with a cooling rate of 2.5 °C·h^{-1}. The suspension was filtered and washed with deionized water. The transparent spherical HMX-DMF complexes with smooth surfaces were obtained. Then, add the obtained spherical HMX-DMF complexes to 500 mL deionized water and heat to 30 °C stirring for 2 h to remove DMF from HMX-DMF complexes. Then, the HMX particles with high specific surface area can be obtained.

2.3. Preparation of HMX@TA-Pb/Cu and HMX@SA-Pb/Cu composites

2.3.1. Preparation of HMX@TA-Pb/Cu composites

At 25 °C, 1.0 g TA and 50 mL deionized water were added into 250 mL three-necks flask and stirred at this temperature until TA is completely dissolved. Then, 10 g HMX particles were added to TA solution and stirred for 30 min to disperse. Then, 180 mg $Cu(NO_3)_2$ and 320 mg $Pb(NO_3)_2$ were added to the above suspension and stirred for 30 min to supply Cu^{2+} and Pb^{2+}. Tris-Bis was then added into the above suspension to adjust the pH value to 7–8. The resulted suspension was stirred at 25 °C for 1 h and then filtered and washed with deionized water. The obtained HMX@TA-Pb/Cu composites were dried in a vacuum oven at 50 °C for 8 h. Repeat above procedures five times to increase the thickness of TA-Pb/Cu.

2.3.2. Preparation of HMX@SA-Pb/Cu composites

At 25 °C, 1.0 g SA and 50 mL deionized water were added into 250 mL three-necks flask and stirred at this temperature until SA is completely dissolved. Then, 10 g HMX particles were added to SA solution and stirred for 30 min to disperse. Then, 180 mg $Cu(NO_3)_2$ and 320 mg $Pb(NO_3)_2$ were added to the above suspension and stirred for 30 min to supply Cu^{2+} and Pb^{2+}. Tris-Bis was then added into the above suspension to adjust the pH value to 6–7. The resulted suspension was stirred at 25 °C for 1 h and then filtered and washed with deionized water. The obtained HMX@SA-Pb/Cu composites were dried in a vacuum oven at 50 °C for 8 h. Repeat above procedures five times to increase the content of SA-Pb/Cu.

2.4. Characterization of HMX@TA-Pb/Cu and HMX@SA-Pb/Cu composites

X-ray photoelectron spectroscopy (XPS), X-ray diffraction (XRD) and Fourier-transform infrared spectra (FT-IR) were used to characterize the structure of HMX@TA-Pb/Cu and HMX@SA-Pb/Cu composites. Scanning electron microscope (SEM) and atomic force microscope (AFM) were used to investigate the surface morphology and surface roughness of HMX@TA-Pb/Cu and HMX@SA-Pb/Cu composites. High-performance liquid chromatography (HPLC) was used to study the content of HMX@TA-Pb/Cu and HMX@SA-Pb/Cu composites. Differential scanning calorimetry (DSC) was used to study the non-isothermal decomposition properties of HMX@TA-Pb/Cu and HMX@SA-Pb/Cu composites. Accelerating rate calorimeter (ARC) was used to study the catalytic effects of TA-Pb/Cu and SA-Pb/Cu on HMX thermal decomposition process. The combustion residues of HMX@TA-Pb/Cu and HMX@SA-Pb/Cu composites are collected and characterized by SEM and energy dispersive spectroscopy (EDS) to further study the catalytic effect of lead/cupric salt shells on combustion.

2.5. Adsorption mechanism of TA-Pb/Cu and SA-Pb/Cu on HMX surface

Molecular dynamics (MD) simulations were performed to analyze the interaction between HMX surface and TA (or SA) layer. The geometry of HMX lattice and TA (or SA) molecule were optimized through COMPASS Ⅱ force field (version 1.2) (Sun, 1998) with energy, force and displacement convergence tolerance of 10^{-4} kcal·mol^{-1}, 0.005 kcal·mol^{-1}·Å^{-1} and 5×10^{-5} Å. The most uneven surface {1 0 0} of HMX was selected to study the interaction between HMX surface and TA (or SA) in this work. 1000 ps MD simulation was conducted in NVT ensemble at 298 K with Andersen thermostat (Andersen, 1980) to search the most stable structure between HMX surface and TA (or SA). The systems were first performed for 500 ps with a time step of 1 fs in the equilibration runs, then followed by the production runs of 500 ps. The electrostatic interaction was calculated by Ewald method with an accuracy of 0.0001 kcal·mol^{-1} (Ewald, 1921), and van der Waals force was computed by the atom based method with the cut-off distance of 15.5 Å (Kitson and Hagler, 1988; Lan et al., 2018; Li et al., 2019). In this study, the dynamic trajectory was recorded every 200 fs, during which the data were collected for subsequent analysis.

3. Results and discussions

3.1. Crystal structure and surface element analysis of HMX@TA-Pb/Cu and HMX@SA-Pb/Cu composites

XRD and FT-IR are adopted to characterize the crystal form and chemical structure of HMX, HMX-DMF, HMX@TA-Pb/Cu and HMX@SA-Pb/Cu. XRD patterns and FT-IR spectra of different samples are summarized in Fig. 2a and Fig. 2b, respectively. The characteristic peaks of XRD and FT-IR of HMX still exist after coating with TA-Pb/Cu and SA-Pb/Cu shells, illustrating that the crystal form and chemical structures of HMX in HMX@TA-Pb/Cu and HMX@SA-Pb/Cu composites are not changed during *in situ* coating process. The characteristic peaks of DMF on FT-IR spectra are disappeared, illustrating that DMF are completely removed from HMX-DMF complex. In addition, the strong response of HMX and low content of TA-Pb/Cu and SA-Pb/Cu shells result in that it is hard to detect the response of TA-Pb/Cu and SA-Pb/Cu in XRD patterns and FT-IR spectra. Therefore, TA-Pb/Cu and SA-Pb/Cu shells have few influences on the detonation properties of HMX, in that the content of TA-Pb/Cu and SA-Pb/Cu are low. The mass content of TA-Pb/Cu and SA-Pb/Cu shells are measured by HPLC, and the mass fraction of TA-Pb/Cu and SA-Pb/Cu are 1.96% and 1.88%, respectively.

XPS is used to analysis the surface element of HMX, HMX@TA-Pb/Cu and HMX@SA-Pb/Cu composites. Full XPS spectra can be used to judge whether TA-Pb/Cu and SA-Pb/Cu have been introduced to HMX surfaces, because the element types of TA-Pb/Cu and SA-Pb/Cu are different with HMX. Full XPS spectra of HMX, HMX@TA-Pb/Cu

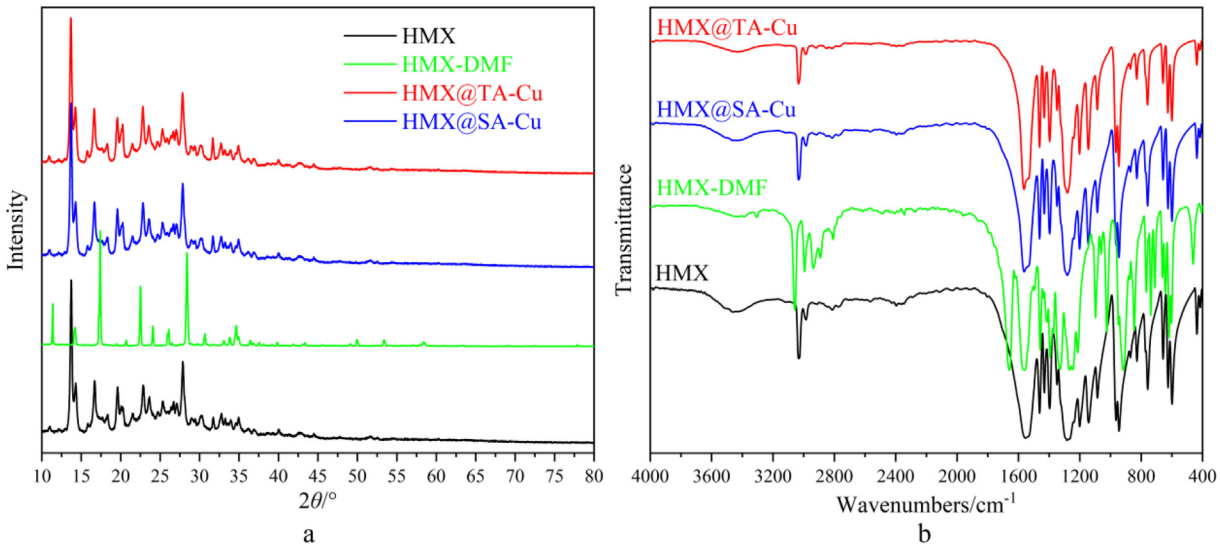

Fig. 2 XRD patterns (a) and FT-IR spectra (b) of HMX, HMX-DMF, HMX@TA-Pb/Cu and HMX@SA-Pb/Cu.

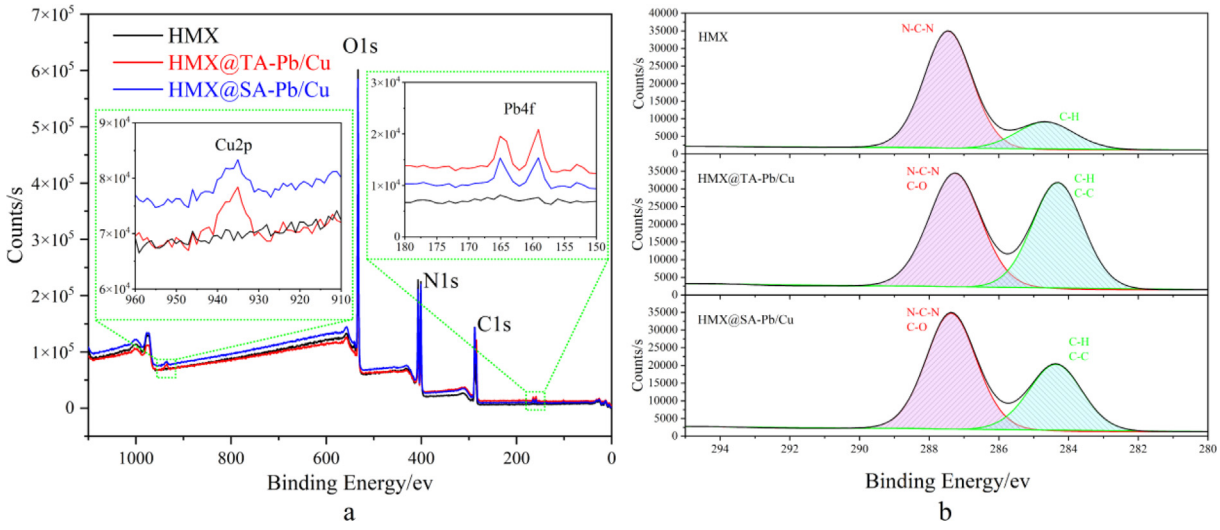

Fig. 3 Full xps spectra (a) and c1s xps spectra (b) of hmx, hmx@ta-pb/cu and hmx@sa-pb/cu.

and HMX@SA-Pb/Cu are listed in Fig. 3a. Compared with pure HMX, Pb4f and Cu2p peaks are detected in HMX@TA-Pb/Cu and HMX@SA-Pb/Cu composites, illustrating that TA-Pb/Cu and SA-Pb/Cu have been introduced to the surface of HMX. In addition, XPS high-resolution spectra of C1s region (Fig. 3b) are used to further evaluate the surface structure of HMX@TA-Pb/Cu and HMX@SA-Pb/Cu. C1s region of HMX can be divided into two peaks, assigned to C–H (284.68 eV) and N-C-N (287.48 eV). Compared with pure HMX, the peak shapes of C1s of HMX@TA-Pb/Cu and HMX@SA-Pb/Cu have some differences. The intensity of the peak around 284 eV are increased because of the introduce of C–C and C–H on HMX surfaces, which further illustrates that TA-Pb/Cu and SA-Pb/Cu are introduced to the surface of HMX. Above all, the emergence of Pb4f and Cu2p peaks and the variation of C1s high-resolution spectra peaks illustrate that TA-Pb/Cu and SA-Pb/Cu have been introduced to HMX surface.

3.2. Surface topographies of HMX@TA-Pb/Cu and HMX@SA-Pb/Cu composites

It can be concluded from XPS results that the surface elements of HMX@TA-Pb/Cu and HMX@SA-Pb/Cu composites are different with pure HMX due to the introduction of TA-Pb/Cu and SA-Pb/Cu shells. In order to view the microstructure of HMX@TA-Pb/Cu and HMX@SA-Pb/Cu composites, SEM and AFM are further used to characterized their surface topographies, and the characterization results are summarized in Fig. 4. It can be seen from Fig. 4a that there are many gullies and holes on HMX particles, which is caused by the removing of DMF from HMX-DMF complexes. The average pore diameter of the pore is 11.2458 nm. The gullies and holes are ideal adsorption sites during *in situ* coprecipitation coating. Fig. 4b and Fig. 4c displays the surface morphology of HMX@TA-Pb/Cu and HMX@SA-Pb/Cu composites, which is obviously different from HMX particles, illustrating that

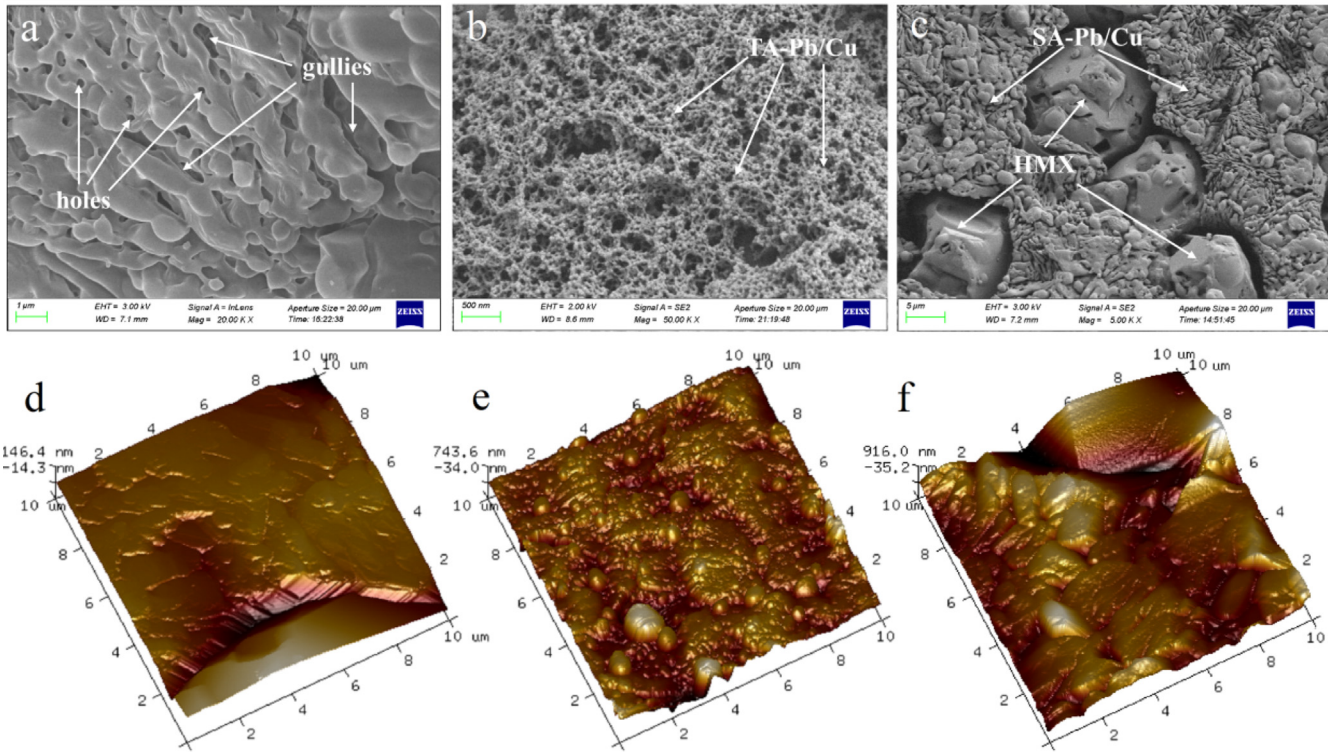

Fig. 4 Surface morphology of HMX particle (a), HMX@TA-Pb/Cu (b) and HMX@SA-Pb/Cu (c). Topographical AFM images of HMX particle (d), HMX@TA-Pb/Cu (e) and HMX@SA-Pb/Cu (f).

TA-Pb/Cu and SA-Pb/Cu are introduced to the surface of HMX. For HMX@TA-Pb/Cu composites, uniform TA-Pb/Cu shells are formed and compactly coated on HMX surfaces, due to the excellent membrane-forming properties of TA. There are twenty-five hydroxyls in TA that can react with Pb^{2+} and Cu^{2+} to form metal-phenolic networks film, but the hydroxyls will not react with Pb^{2+} and Cu^{2+} completely. The unreacted hydroxyls will form hydrogen bonds with HMX surface and thus coating HMX well. In addition, coralloid TA-Pb/Cu shells can further increase the specific surface area of samples, resulting in a significant improvement of accessible area and thus a significant improvement of mechanical properties and combustion properties. For HMX@SA-Pb/Cu composites, SA-Pb/Cu particles are deposition into the gullies and holes of HMX surfaces. Some HMX surfaces are still exposed due to SA-Pb/Cu particles can not form continuous film. There are only one hydroxyl and one carboxyl in SA that can react with Pb^{2+} and Cu^{2+}. In addition, SA-Pb/Cu particles will immediately precipitate and deposition into the gullies or holes of HMX surface, when hydroxyl or carboxyl react with Pb^{2+} and Cu^{2+}. With the deposition going on, the gullies and holes of HMX surface are gradually filled up. The surface structure of HMX@TA-Pb/Cu and HMX@SA-Pb/Cu are much different, resulting in that the performance of HMX@TA-Pb/Cu and HMX@SA-Pb/Cu may different. In addition, when the energy of electron beam is high, HMX surface easily crack and become wrinkled, while the surface of HMX@TA-Pb/Cu and HMX@SA-Pb/Cu composites are much stabler under the same condition, indicating that HMX surfaces become obviously resistant to electronic beam under protection of TA-Pb/Cu and SA-Pb/Cu. AFM topographical image of HMX@TA-Pb/Cu (Fig. 4e) and HMX@SA-Pb/Cu (Fig. 4f) have great differences from HMX particle (Fig. 4d), which further illustrates that TA-Pb/Cu and SA-Pb/Cu are introduced to the surface of HMX. Compared with HMX particles, the mean value of roughness (R_a) of HMX@TA-Pb/Cu and HMX@SA-Pb/Cu increase from 31.4 nm to 549 nm and 628 nm, because of the deposition and adsorption of TA-Pb/Cu and SA-Pb/Cu. Both AFM and SEM images show TA-Pb/Cu and SA-Pb/Cu are formed on the surface of HMX, and the roughness are remarkedly increased after *in situ* coating. Such improvement in surface roughness provides an additional benefit to the adhesion of HMX crystals in energetic composites, which can be utilized for further practical applications.

3.3. Adsorption mechanism of TA-Pb/Cu and SA-Pb/Cu on HMX surface

In statistical mechanics, radial distribution function (RDF) in a system of particles (atoms, molecules, colloids, etc.) describes how density varies as a function of distance from a reference particle (Lan et al., 2018). The RDF analysis can be used to analyze the contribution of hydrogen bonds, van der Waals forces and electrostatic interactions on the total interaction between HMX surface and TA (or SA). Generally, the distance ranges of hydrogen bonding interactions, van der Waals interactions and electrostatic interactions are within 3.1 Å, 3.1–5.0 Å and beyond 5.0 Å, respectively (Lan et al., 2018; Lu and Chen, 2012). The RDF diagram between HMX and TA is displayed in Fig. 5a, The RDF diagram between HMX and SA is displayed in Fig. 5b.

It can be seen from Fig. 5a that there are two peaks on the RDF curve of HMX-NO_2-O ~ TA-OH-H, within 3.1 Å

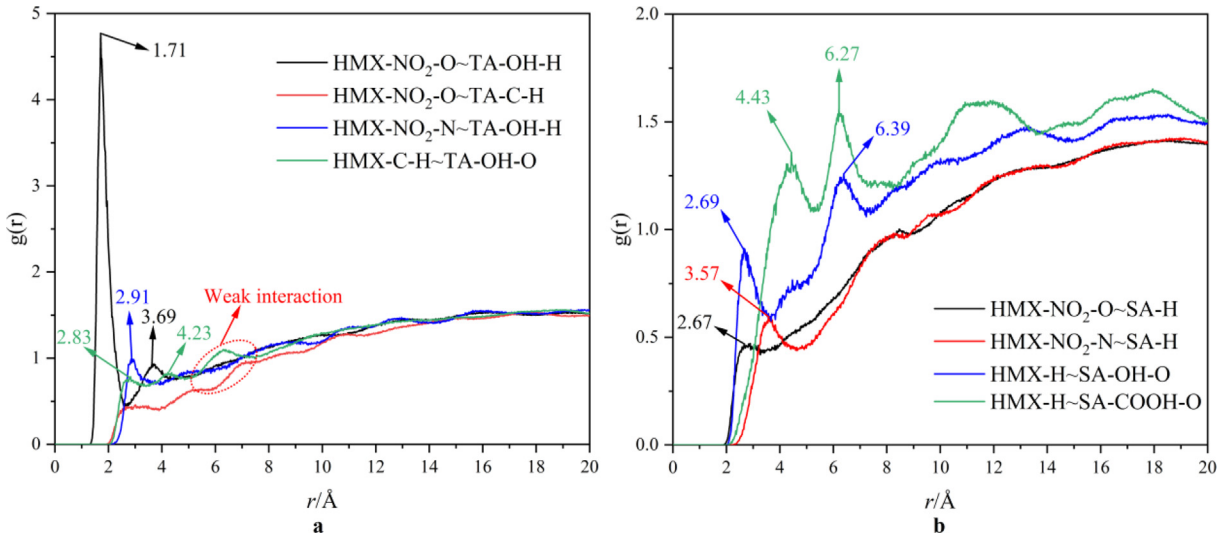

Fig. 5 A rdf diagram between HMX and TA, b RDF diagram between HMX and SA.

and 3.1–5.0 Å, respectively, illustrating that hydrogen bonds and van der Waals forces exist between oxygen atom of the nitro group of HMX and hydrogen atom of phenolic hydroxyl group of TA. The hydrogen bonds are strong, because the peak within 3.1 Å is stronger than other peaks. Within 3.1 Å, the RDF curve of HMX-NO_2-N ~ TA-OH-H and HMX-H ~ TA-OH-O emerge weak peaks, illustrating that hydrogen bonds may exist between these atoms. In addition, some weak peaks exist beyond 5.0 Å, illustrating electrostatic interaction exists in this system. Moreover, the intensity is much larger for the peak on HMX-NO_2-O ~ TA-OH-H RDF curve within 3.1 Å, which indicates that the interactions between TA and HMX surface are mainly contributed by the hydrogen bonds between TA-OH-H and HMX-NO_2-O. Strong hydrogen bonds of HMX-NO_2-O ~ TA-OH-H result in high interaction between TA and HMX surface, and thus good coating effects of TA on HMX. Fig. 5b illustrates that hydrogen bonds, van der Waals forces and electrostatic interaction may exist between HMX and SA, in that some peaks exist on RDF curve within 3.1 Å, 3.1–5.0 Å and beyond 5.0 Å, respectively. The intensity of each peak is close and weak, illustrating that the contribution of hydrogen bonds, van der Waals forces and electrostatic interaction are close and weak. The weak interaction between HMX and SA results in that SA-Pb/Cu particles are difficulty to adsorb on HMX surface. Comparing with HMX@SA-Pb/Cu, the interaction between HMX and TA is higher, and thus the TA-Pb/Cu can easily coat on HMX surface while SA-Pb/Cu can only deposit in the gullies and holes of HMX surface.

3.4. Mechanical and thermal sensitivities of HMX@TA-Pb/Cu and HMX@SA-Pb/Cu composites

XPS, SEM and AFM results show that TA-Pb/Cu and SA-Pb/Cu have been introduced to HMX surfaces. In order to evaluate the effects of TA-Pb/Cu and SA-Pb/Cu on mechanical and thermal sensitivities of HMX, the impact sensitivity, friction sensitivity and explosion point (5 s delay method) of raw HMX, HMX particles with high specific surface area, HMX@TA-Pb/Cu and HMX@SA-Pb/Cu are measured according to GJB 772A (GJB 772A, 1997). The obtained results are summarized in Table 1.

Table 1 illustrate that the mechanical sensitivities of HMX@TA-Pb/Cu are lower than that of raw HMX and HMX particles due to the protection of TA-Pb/Cu shells. An extraordinarily high coverage and hard TA-Pb/Cu shell is generated on HMX surfaces via *in situ* coprecipitation coating technique. High strength TA-Pb/Cu shells endow HMX particles hard armours that can protect HMX crystals when suffering external mechanical stimulations and thus decrease the mechanical sensitivities. The coralloid TA-Pb/Cu shells can deform greatly and thus cushion the external mechanical stimulations, resulting in the mechanical sensitivity of HMX@TA-Pb/Cu composites are low. Compared with raw HMX and HMX particles, the mechanical sensitivities of HMX@SA-Pb/Cu are decreased as well, in that the non-explosive component SA-Pb/Cu can share some stress when suffering external mechanical stimulations. SA-Pb/Cu embedded in the gullies and holes of HMX can decrease the collision probability between HMX, which can decrease the probability of hot spot formation. The mechanical sensitivities of HMX@TA-Pb/Cu are lower than HMX@SA-Pb/Cu, because of the higher coverage of TA-Pb/Cu and no HMX exposed. Compared with raw HMX and HMX particles, the explosion points of HMX@TA-Pb/Cu and HMX@SA-Pb/Cu are increased, illustrating that the thermal safeties of HMX@TA-Pb/Cu and HMX@SA-Pb/Cu are increased. For coralloid TA-Pb/Cu shells, there are many gases with low thermal conductive in the pore, which can decline the heat transportation rate and thus increase explosion points. For HMX@SA-Pb/Cu composites, the heat generate by HMX thermal decomposition can transport to SA-Pb/Cu and thus decrease heat accumulation, resulting in higher explosion points. Above all, the mechanical and thermal safeties of HMX can be obviously enhanced by TA-Pb/Cu and SA-Pb/Cu.

3.5. Non-isothermal decomposition of HMX@TA-Pb/Cu and HMX@SA-Pb/Cu composites

The introduction of TA-Pb/Cu and SA-Pb/Cu may affect the non-isothermal decomposition properties of HMX. DSC mea-

Table 1 Impact sensitivity, friction sensitivity and explosion point of raw HMX, HMX particles, HMX@TA-Pb/Cu and HMX@SA-Pb/Cu.

parameters	raw HMX	HMX particles	HMX@TA-Pb/Cu	HMX@SA-Pb/Cu
impact sensitivity/%	100	84	48	72
friction sensitivity/%	100	88	56	80
explosion point/°C	304	309	323	314

surements are performed at different heating rate with nitrogen atmosphere to evaluate the effects of TA-Pb/Cu and SA-Pb/Cu on the non-isothermal decomposition properties of HMX@TA-Pb/Cu and HMX@SA-Pb/Cu composites. In addition, the non-isothermal decomposition properties of HMX/TA-Pb/Cu and HMX/SA-Pb/Cu physical mixtures are measured by DSC as well. The mass fraction of TA-Pb/Cu and SA-Pb/Cu of physical mixtures are 2%, which are the same with that of HMX@TA-Pb/Cu and HMX@SA-Pb/Cu composites. The obtained DSC results of different samples at a heating rate of 10 °C·min^{-1} are summarized in Fig. 6a and Fig. 6b. The decomposition temperature (T_p) of different samples at different heating rate are summarized in Table 2. Based on DSC results, the activation energy is obtained by Kissinger and Ozawa methods (Kissinger, 1957; Ozawa, 1965).

Compared with pure HMX and HMX particles, there is no significant change in phase transition temperature (T_t), melting point (T_m) and decomposition temperature (T_p) of different physical mixtures, illustrating that physical mixing has few influences on non-isothermal decomposition properties of HMX. Compared with pure HMX, the T_t of HMX@TA-Pb/Cu composites increase from 191.17 °C to 201.83 °C, while T_t of HMX@SA-Pb/Cu composites decrease from 191.17 °C to 174.50 °C. These phenomena illustrate that TA-Pb/Cu shell can enhance the stabilization of β-HMX due to the low thermal conductivity and high decomposition temperature of TA-Pb/Cu shell, while SA-Pb/Cu can catalyze the phase transition process of β-HMX due to the molecule structure of SA-Pb/Cu is small and Pb/Cu can easily contact with HMX. In addition, DSC did not detect the melting process of HMX@TA-Pb/Cu composites, due to the high coverage and heat insulation of TA-Pb/Cu shell. There is no significant change in T_m of HMX@SA-Pb/Cu composites, demonstrating that SA-Pb/Cu has few influences on the melting process of HMX. The initial decomposition temperature of HMX@TA-Pb/Cu and HMX@SA-Pb/Cu composites are close to that of pure HMX, illustrating that TA-Pb/Cu and SA-Pb/Cu have few influences on thermal stability of HMX. The full width at half-maximum of decomposition peak decreases from 5.33 °C to 4.51 °C and 3.75 °C for HMX@TA-Pb/Cu and HMX@SA-Pb/Cu, illustrating that the decomposition rate of HMX is increased due to the introduction of lead and copper. The activating energy are decrease after coating with TA-Pb/Cu or SA-Pb/Cu shells, which further illustrates that Pb/Cu shells can catalyze the non-isothermal decomposition of HMX. In addition, the catalytic effect of SA-Pb/Cu is better than that of TA-Pb/Cu, because the contents of lead and copper in SA-Pb/Cu is higher than that of TA-Pb/Cu. The full width at half-maximum of HMX/TA-Pb/Cu and HMX/SA-Pb/Cu physical mixtures have few variations with HMX, demonstrating that the catalytic effect of TA-Pb/Cu and SA-Pb/Cu can not be sufficiently exploited by physical mixing. Above all, TA-Pb/Cu shells can enhance the stabilization of β-HMX and catalyze the non-isothermal decomposition of HMX. SA-Pb/Cu can catalyze the phase transition process of β-HMX and catalyze the non-isothermal decomposition

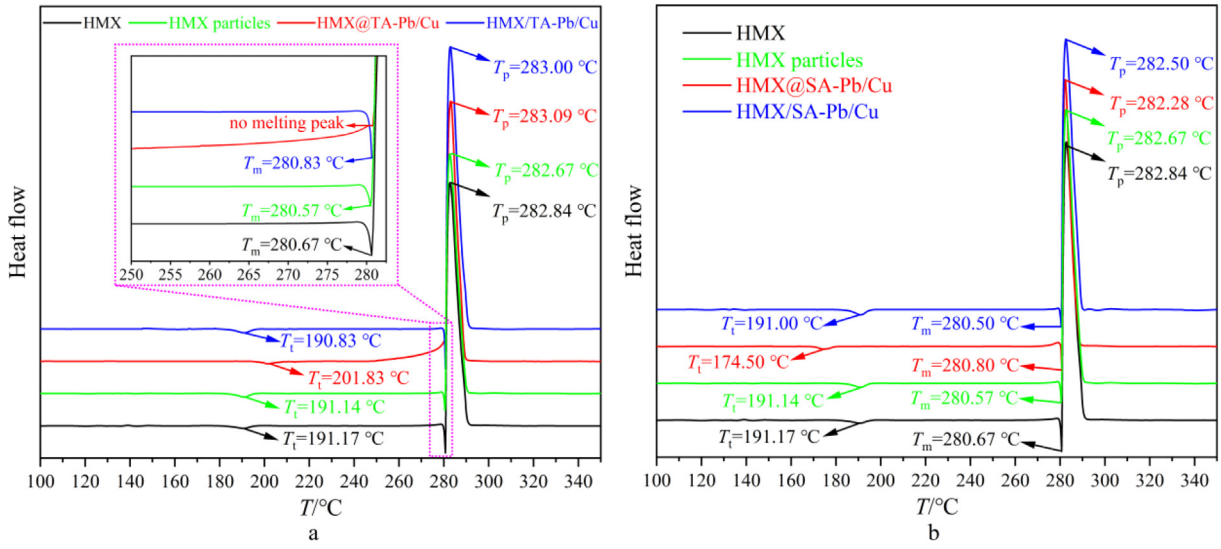

Fig. 6 A dsc results of hmx, hmx-dmf, hmx@ta-pb/cu composites and hmx/ta-pb/cu physical mixtures, b dsc results of hmx, hmx-dmf, hmx@sa-pb/cu composites and hmx/sa-pb/cu physical mixtures.

Table 2 The decomposition temperature and activating energy of different samples.

heating rate/°C·min^{-1}	T_p/°C				
	HMX	HMX@TA-Pb/Cu	HMX/TA-Pb/Cu	HMX@SA-Pb/Cu	HMX/SA-Pb/Cu
5	278.54	278.91	278.62	279.08	279.13
10	282.84	283.09	283.00	282.28	282.50
15	284.35	284.66	284.40	284.75	284.59
20	285.27	286.10	285.66	286.33	286.45
E_a/(kJ·mol^{-1})	493.15	477.39	480.84	470.82	474.68

of HMX. Compared with physical mixing, the catalytic effect of Pb/Cu can be exploited more sufficiently through *in situ* coprecipitation technics.

3.6. Catalytic effects of TA-Pb/Cu and SA-Pb/Cu on HMX

Non-isothermal decomposition results illustrate that TA-Pb/Cu and SA-Pb/Cu can catalyze the thermal decomposition process of HMX, but the catalytic effect of TA-Pb/Cu and SA-Pb/Cu are unclear. Heat-wait-search (HWS) procedure of ARC is used to further study the catalytic effects of TA-Pb/Cu and SA-Pb/Cu on thermal decomposition of HMX (Lan et al., 2020; Li et al., 2021). As comparisons, the adiabatic thermal decomposition performances of HMX/TA-Pb/Cu and HMX/SA-Pb/Cu physical mixtures are studied by ARC as well. 120 ± 1 mg samples are used to perform the HWS procedure with temperature increment of 5 °C. The obtained exothermic processes of different samples are summarized in Fig. 7. The obtained initial decomposition temperature (T_0), initial decomposition time (t_0), final decomposition temperature (T_f), final decomposition time (t_f), adiabatic temperature rise (ΔT_{ad}) and whole decomposition period (Δt) are listed in Table 3.

Compared with pure HMX, the T_0 of HMX@TA-Pb/Cu and HMX@SA-Pb/Cu composites increases from 225.65 °C to 230.24 °C and 233.26 °C, while the T_0 of HMX/TA-Pb/Cu and HMX/SA-Pb/Cu physical mixtures have few variations, demonstrating that *in situ* coprecipitation technics can enhance the adiabatic stability of HMX and physical mixings have few influences on the adiabatic stability of HMX. Compared with pure HMX, the decomposition period (Δt) of HMX@TA-Pb/Cu, HMX/TA-Pb/Cu, HMX@SA-Pb/Cu and HMX/SA-Pb/Cu decrease from 28.88 min to 7.04 min, 10.24 min, 4.59 min and 9.97·min, respectively, illustrating that TA-Pb/Cu and SA-Pb/Cu can catalyze thermal decomposition of HMX. In addition, the Δt of composites are shorter than that of physical mixtures, illustrating that the catalytic effects of Pb/Cu cannot be exploited sufficiently through physical mixing. For HMX@TA-Pb/Cu and HMX@SA-Pb/Cu composites, the Pb/Cu are closely adsorbed on the gullies and holes of HMX surface. When HMX@TA-Pb/Cu and HMX@SA-Pb/Cu suffer thermal stimulations, the effective catalytic component (PbO/CuO) will generate by TA-Pb/Cu and SA-Pb/Cu. The generated PbO/CuO will closely attach to HMX and catalyze the decomposition of HMX. Compared with pure HMX, the ΔT_{ad} of HMX@TA-Pb/Cu, HMX/TA-Pb/Cu, HMX@SA-Pb/Cu and HMX/SA-Pb/Cu increase from 29.50 °C to 31.46 °C, 31.93 °C, 34.32 °C and 30.63·°C, illustrating that Pb/Cu can make the decomposition of HMX more complete, and thus release more heat. Above all, *in situ* coprecipitation technics can enhance the adiabatic stability of HMX, while physical mixings have few influences on the adia-

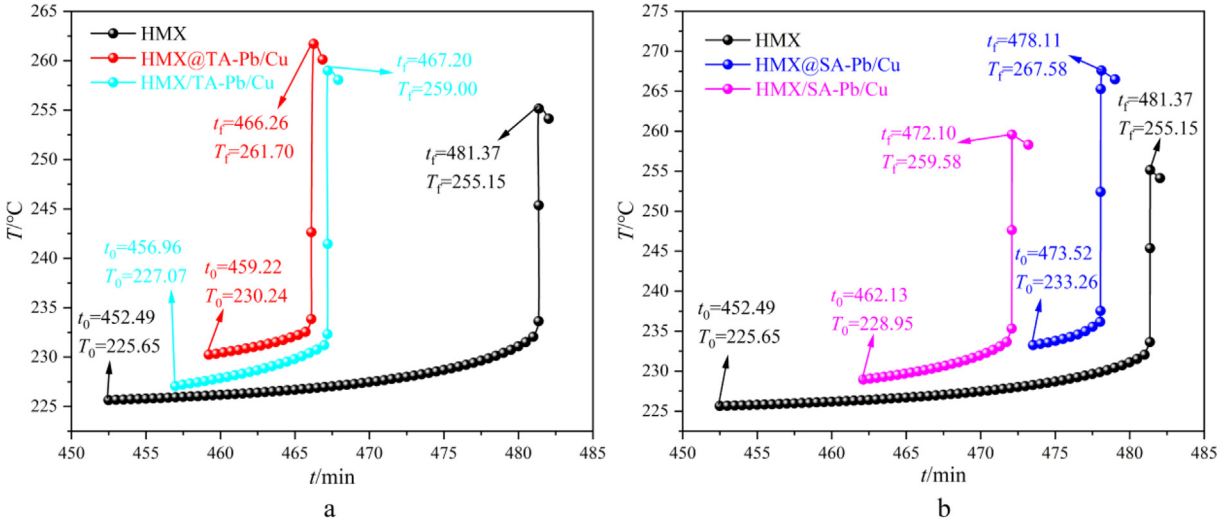

Fig. 7 A arc results of hmx, hmx@ta-pb/cu composites and hmx/ta-pb/cu physical mixtures, b arc results of hmx, hmx@sa-pb/cu composites and hmx/sa-pb/cu physical mixtures.

Table 3 Adiabatic thermal decomposition parameters of HMX, HMX@TA-Pb/Cu, HMX/TA-Pb/Cu, HMX@SA-Pb/Cu, HMX/SA-Pb/Cu.

parameters	HMX	HMX@TA-Pb/Cu	HMX/TA-Pb/Cu	HMX@SA-Pb/Cu	HMX/SA-Pb/Cu
sample mass/g	0.1202	0.1207	0.1204	0.1202	0.1205
T_0/°C	225.65	230.24	227.07	233.26	228.95
t_0/min	452.49	459.22	456.96	473.52	462.13
T_f/°C	255.15	261.70	259.00	267.58	259.58
t_f/min	481.37	466.26	467.20	478.11	472.10
ΔT_{ad}/°C	29.50	31.46	31.93	34.32	30.63
Δt/min	28.88	7.04	10.24	4.59	9.97

batic stability of HMX. Both physical mixing and *in situ* coprecipitation can catalyze the thermal decomposition process of HMX, while the catalytic effects of *in situ* coprecipitation technics are better than that of physical mixings.

In order to study the catalytic effect of TA-Pb/Cu and SA-Pb/Cu on HMX combustion performances, HMX, HMX@TA-Pb/Cu, HMX/TA-Pb/Cu, HMX@SA-Pb/Cu and HMX/SA-Pb/Cu are combusted in air atmosphere, and the solid residues after combustion are collected for further SEM and EDS analyses. The obtained SEM and EDS results are summarized in Fig. 8 and Fig. 9 respectively. Fig. 8 shows that porous structure Pb/Cu oxides residues are obtained after HMX@TA-Pb/Cu and HMX@SA-Pb/Cu composites combusted, and the porous structure residues are distributed in the residues. For HMX/TA-Pb/Cu and HMX/SA-Pb/Cu physical mixtures, the distribution of Pb/Cu oxides are centered in some locals. These phenomena illustrate that the combustion results of composites are better than physical mixtures. Fig. 9 shows that Au peak is detected in EDS results, because each sample is treated by spraying gold before EDS measurement. The total peak area of C, N and O of physical mixtures and composites are smaller than that of pure HMX, illustrating that the combustion is more sufficiently due to the catalysis of Pb/Cu. In addition, the total peak area of C, N and O of HMX@TA-Pb/Cu and HMX@SA-Pb/Cu composites are lower than that of physical mixture, illustrating that the catalytic effects of *in situ* coprecipitation is better than physical mixing.

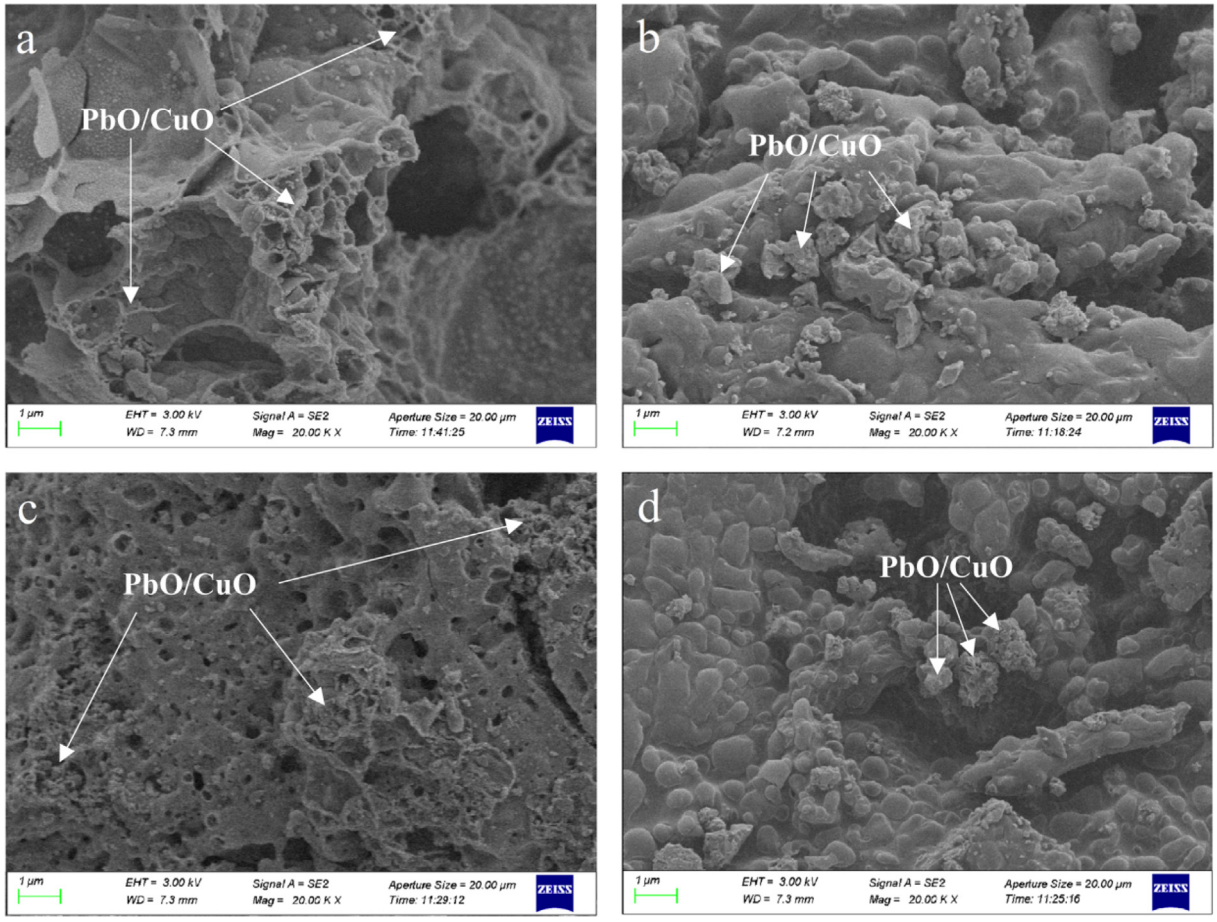

Fig. 8 SEM images of the residues of HMX@TA-Pb/Cu (a), HMX/TA-Pb/Cu (b), HMX@SA-Pb/Cu (c) and HMX/SA-Pb/Cu (d).

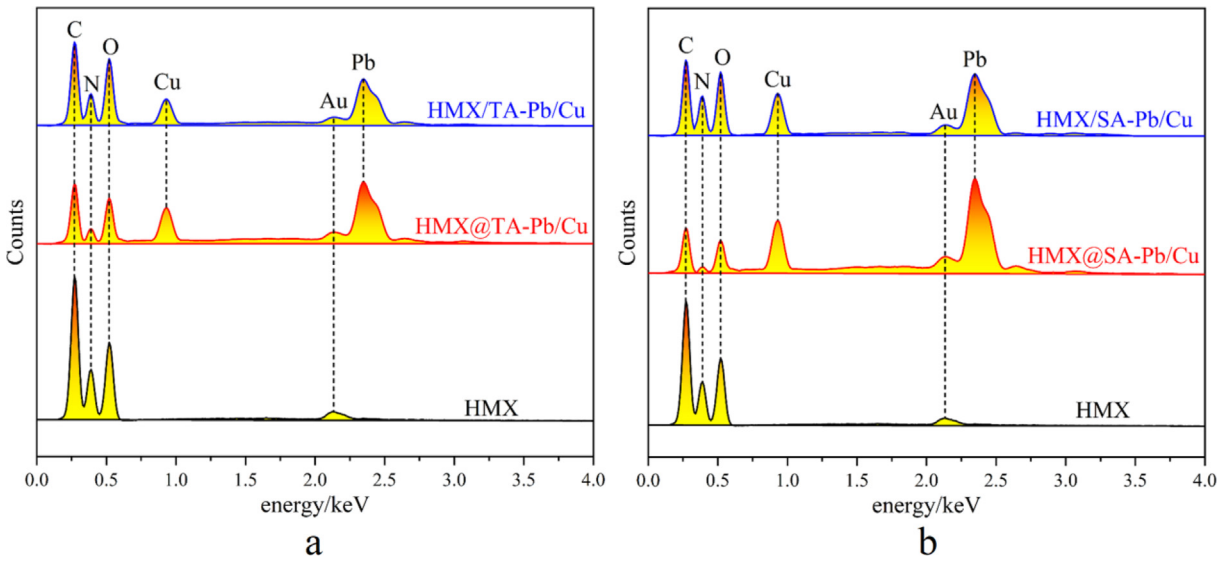

Fig. 9 A eds spectra of the residues of hmx, hmx@ta-pb/cu and hmx/ta-pb/cu, b eds spectra of the residues of hmx, hmx@sa-pb/cu and hmx/sa-pb/cu.

4. Conclusions

HMX@TA-Pb/Cu and HMX@SA-Pb/Cu composites are prepared via *in situ* coprecipitation technics. XRD and FT-IR results show that the physical and chemical structures of HMX have not changed during *in situ* coprecipitation process. XPS, SEM and AFM results show that TA-Pb/Cu and SA-Pb/Cu have been successfully introduced to HMX surface due to the strong hydrogen bond between HMX and TA or SA, among which TA-Pb/Cu shells are uniform coated to HMX surface while SA-Pb/Cu particles are embedded in the gullies and holes of HMX. The mechanical and thermal sensitivities of HMX@TA-Pb/Cu and HMX@SA-Pb/Cu composites is lower than HMX, because of the protection of TA-Pb/Cu and SA-Pb/Cu. TA-Pb/Cu can enhance the stabilization of β-HMX, while SA-Pb/Cu can catalyze the phase transition process of β-HMX. TA-Pb/Cu and SA-Pb/Cu can catalyze the decomposition and combustion of HMX, and the catalytic effects of Pb/Cu are better through *in situ* coprecipitation than physical mixing.

Conflict of interest

No conflict of interest exits in the submission of this manuscript, and manuscript is approved by all authors for publication.

Acknowledgments

This work was supported by Fundamental Research Program of Shanxi Province (Grant No. 202103021223192).

References

An, C.W., Li, H.Q., Guo, W.J., Geng, X.H., Wang, J.Y., 2014. Nano cyclotetramethylene tetranitramine particles prepared by a green recrystallization process. Propell. Explos. Pyrot. 39, 701–706.

Andersen, H.C., 1980. Molecular dynamics simulations at constant pressure and/or temperature. J. Chem. Phys. 72, 2374–2383.

Bolton, O., Matzger, A.J., 2011. Improved stability and smart-material functionality realized in an energetic cocrystal. Angew. Chem. Int. Ed. 50, 8960–8963.

Cobbledick, R.E., Small, R.W.H., 1975. The crystal structure of the complex formed between 1,3,5,7-tetranitro-l,3,5,7-tetraazaeyclooetane (HMX) and *N*, N-dimethylformamide (DMF). Acta Cryst. 31, 2805–2808.

Elbasuney, S., Ismael, S., Yehia, M. Ammonium percholorate/HMX co-crystal: bespoke energetic materials with tailored decomposition kinetics via dual catalytic effect, J. Energ. Mater. doi: 10.1080/07370652.2021.1982071.

Ewald, P.P., 1921. Evaluation of optical and electrostatic lattice potentials. Ann. Phys. 64, 253–287.

GJB 772A, Explosive test method, Beijing, China Weapons Industry Press, 1997.

Gong, F.Y., Zhang, J.H., Ding, L., Yang, Z.J., Liu, X.B., 2017. Mussel-inspired coating of energetic crystals: A compact core-shell structure with highly enhanced thermal stability. Chem. Eng. J. 309, 140–150.

Hou, C.H., Zhang, Y.P., Chen, Y.G., Jia, X.L., Zhang, S.M., Tan, Y. X., 2018. Fabrication of ultra-fine TATB/HMX cocrystal using a compound solvent. Propell. Explos. Pyrot. 43, 916–922.

Jiang, Q., Luo, Y., Yang, F., Ju, R., Zhang, M., Wang, W., Li, B., 2020. Influence of lead and copper salt catalysts on the thermal decomposition and cook-off responses of DNTF. Chin. J. Energ. Mater. 28, 470–474.

Kissinger, H.E., 1957. Reaction kinetics in differential thermal analysis. Anal. Chem. 29, 1702–1706.

Kitson, D.H., Hagler, A.T., 1988. Theoretical studies of the structure and molecular dynamics of a peptide crystal. Biochemistry 27, 5246–5257.

Klapötke, T.M., 2018. Energetic Materials Encyclopedia. De Gruyter, Berlin.

Kosareva, E.K., Zharkov, M.N., Meerov, D.B., Gainutdinov, R.V., Fomenkov, I.V., Zlotin, S.G., Pivkina, A.N., Kuchurov, I.V., Muravyev, N.V., 2022. HMX surface modification with polymers via sc-CO_2 antisolvent process: A way to safe and easy-to-handle energetic materials. Chem. Eng. J. 428, 131363.

Lan, G., Jin, S., Li, J., Wang, J., Li, J., Chen, S., Li, L., 2018. The study of external growth environments on the crystal morphology of ε-HNIW by molecular dynamics simulation. J. Mater. Sci. 53, 12921–12936.

Lan, G., Jin, S., Chen, M., Li, J., Lu, Z., Wang, N., Li, L., 2020. Preparation and performances characterization of HNIW/NTO-based high-energetic low vulnerable polymer-bonded explosive. J. Therm. Anal. Calorim. 139, 3589–3602.

Lan, G., Zhang, G., Chao, H., Li, Z., Wang, J., 2022. Jing Li, Ameliorating the performances of 3,4-bis(4′ -nitrofurazano-3′ -yl)furoxan (DNTF) by establishing tannic acid (TA) interface layer on DNTF surface. Chem. Eng. J. 434, 134513.

Li, J., Jin, S.H., Lan, G.C., Xu, Z.S., Wang, L.T., Wang, N., Li, L.J., 2019. Research on the glass transition temperature and mechanical properties of poly(vinyl chloride)/dioctyl phthalate (PVC/DOP) blends by molecular dynamics simulations. Chin. J. Polym. Sci. 37, 834–840.

Li, J., Jin, S., Bao, F., Lan, G., Wang, X., Shu, Q., Lu, B., Chen, K., 2021. Thermal safety assessment and thermo-kinetic parameters of 5,5'-dinitramino-3,3'-bi[1,2,4-triazolate] carbohydrazide salt (CBNT). J. Therm. Anal. Calorim. 144, 647–655.

Li, Z., Zhao, X., Gong, F., Lin, C., Liu, Y., Yang, Z., Nie, F., 2020. Multilayer deposition of metal-phenolic networks for coating of energetic crystals: modulated surface structures and highly enhanced thermal stability. ACS Appl. Energy Mater. 3, 11091–11098.

Lin, C.M., Gong, F.Y., Yang, Z.J., Zhao, X., Li, Y.B., Zeng, C.C., Li, J., Guo, S.Y., 2019. Core-shell structured HMX@polydopamine energetic microspheres: synergistically enhanced mechanical, thermal, and safety performances, polymers 11, 568.

Liu, S., Du, B., Zhang, J., Pan, B., Li, W., Xie, G., 2001. Applied studies of new energetic catalysts in the screw extruded energetic propellant with low signature. Chin. J. Energ. Mater. 9, 130–131.

Lu, T., Chen, F., 2012. Multiwfn: A multifunctional wavefunction analyzer. J. Comput. Chem. 33, 580–592.

Niu, Q., Wang, Q., Chang, T., Li, X., Yin, X., 2022. Preparation of lead-copper complex salt of p-aminosalicylic acid and its influence on propellant performance. Chem. Propell. Polym. Mater. 20, 33–38.

Ozawa, T., 1965. A new method of analyzing thermogravimetric data. B. Chem. Soc. JPN. 38, 1881–1886.

Ren, T., 1994. Nitramine and nitrate ester explosives technology. China Weapons Industry Press, Beijing.

Sun, H., 1998. An ab initio force-field optimized for condensedphase applications overview with details on alkane and benzene compounds. J. Phys. Chem. B 102, 7338–7364.

Xiao, F., Liang, T., 2021. Preparation of hierarchical core-shell Al-PTFE@TA and Al-PTFE@TA-Fe architecture for improving the combustion and ignition properties of aluminum. Surf. Coat. Tech. 412, 127073.

Xiao, F., Liu, Z., Liang, T., Yang, R., Li, J., Luo, P., 2021. Establishing the interface layer on the aluminum surface through the self-assembly of tannic acid (TA): Improving the ignition and combustion properties of aluminum. Chem. Eng. J. 420, 130523.

Yang, Z., Ding, L., Wu, P., Liu, Y., Nie, F., Huang, F., 2015. Fabrication of RDX, HMX and CL-20 based microcapsules via in situ polymerization of melamineformaldehyde resins with reduced sensitivity. Chem. Eng. J. 268, 60–66.